Advanced Ceramics Progress

Research Article

Experimental and Numerical Evaluation of Diffusion Welding of 7075 Aluminum and AZ31 Magnesium Alloys

S. Manafi [a] *, A. Azizi [b]

[a] Department of Materials Engineering, Shahrood Branch, Islamic Azad University, Shahrood, Semnan, Iran
[b] Department of Mechanical Engineering, Faculty of Engineering, Ilam University, Ilam, Ilam, Iran

ARTICLE INFO

ABSTRACT

In the present study, AZ31 magnesium alloy was bonded to 7075 aluminum alloy at different temperatures (393, 402, 412, and 421 °C) and diffrent holding times (25, 60, and 120 min) through diffusion bonding. Moreover, axial loads of 12, 29, 38, and 80 MPa accompanied by vacuum condition were employed during the bonding. The experimental and numerical results of the successful joints confirmed the existence of different reactive layers in diffusion zones and formation of the predicted intermetallic compounds. Findings showed that by applying a pressure of 29 MPa at different temperatures of 402, 412, and 421 °C, Interfacial Transition Zone (ITZ) with thicknesses of 21.26, 21.96, and 22.60 μm, respectively, was formed. Further, the maximum amount of the bond strength (30 MPa), resulting from the proper coalescence of metal surfaces, was obtained at 402 °C. Although the hardness of ITZ was found to be greater than that of the base metals, it could increase even more mainly as a result of an increase in the bonding temperature. Moreover, the results of simulation, using DEFORM-3D software, indicated that the ITZ had different mechanical properties from base metals and that by analyzing the effective stress, the Mg alloy specimen was more deformed than Al alloy during the joining process.

1. INTRODUCTION

It is in the earth crust that one can aboundantly find aluminum and magnesium. In this regard, magnesium (Mg) and aluminum (Al) alloys, in view of their great advantages, namely machinability, good damping properties, low density, dimensional stability, and low cost, attracted great attention in the academic research and industrial applications [1, 2]. Structural components made from Mg and Al alloys are significant industrial materials empolyed in the aerospace and transportation.

Diffusion welding is a solid-state welding process resulting from the application of heat and pressure. In this respect, solid-state diffusion and coalescence phenomenon usually occur in a controlled atmosphere with sufficient time. The process temperature usually ranges from the melting temperatures of 0.5 to 0.8 and accordingly, little plastic deformation occurs during the

process [2]. Due to the formation of fewer unwanted phases in the welding zone, this welding method is of considerable significance compared to traditional welding methods [3, 4]. Some fusion welding defects such as cracking, segregation, and distortion can be avoided using diffusion bonding technology [5]. The most significant effect of the process on designing and manufacturing the industrial parts is clearly observed due to its ability of bonding both similar and dissimilar materials [6].

Welding of dissimilar materials, such as Mg and Al alloys, would result in reducing the wieght and achieving high efficiency in terms of production by substituting Mg and Al alloys for steels [7]. Nevertheless, in order to easily join the alloys, the diffusion bonding process can be employed to make a suitable and strong bonding among them [8, 9].

---

http://www.acerp.ir/article_127892.html

A limited number of research studies have been conducted on modeling the diffusion welding process so far. For instance, Samanta, et al. [10] studied the atomistic simulation of diffusion bonding of dissimilar materials (Al/Cu). In this respect, a numerical approach was proposed in which molecular dynamics were combined with hierarchical calculations to predict the thickness of the diffusion layer. In another study, thermal analysis of copper-aluminum welding was performed using the finite element approach. It was stated that the thermal expansion created during the process would cause thermal residual stress in the joint area [11]. In another attempt, the thermal residual stress in the welding zone was investigated during Al/Mg diffusion bonding, the results of which revealed that the residual stress droped sharply just a short distance from the bonding interface [12].

Generally, a great deal of recent attention has been drawn to the direct application of the diffusion welding process of dissimilar materials, in which an interlayer was not employed, the plastic deformation was minimized, and joint strength increased [13]. Although 7075 aluminum alloy is widely used in advanced industries, less effort has been made to investigate the Al 7075/MgAZ31 diffusion welding in the literature. The simulation of the diffusion welding process can be used as a convenient solution to better understand the process at a lower cost and less time. To this end, the present study aimed to investigate the bonding of 7075 aluminum and AZ31 magnesium alloys using the diffusion welding process at adequate presure, temperature, and holding time in the absence of an interlayer. Moreover, the microstructural and mechanical properties were utilized to investigate the property of the joint. In the following, Al7075/MgAZ31 diffusion welding simulation is developed and discussed. This study can be further referred to as an experimental reference and simulation for dissimilar Al7075/MgAZ31 welding.

2. EXPERIMENTAL PROCEDURES

Square-shaped specimens (13mm × 13mm) with a thickness of 5 mm were machined from magnesium (AZ31B) and aluminum (AA7075T6) alloys. Chemical analysis of raw materials is presented in Table 1.

TABLE 1. Chemical composition of base metals (wt. %)

Alloy Type	Al	Zn	Mn	Cr	Cu	Fe	Ti	Si	Mg
AZ31		3.17	1.1	0.2	-	0.03	0.004	-	0.15	Bal.
Al 7075	Bal.	5.6	0.15	0.2	1.5	0.45	0.03	0.15	2.6

In this respect, to generate the surface roughness, sandpaper number 600# for magnesium and number 1500# for aluminum was used. To remove the impurity before testing the surface, the samples were ultrasonically cleaned in an acetone bath for 15 minutes. Then, the process continued through ethanol 96 and then, the samples were dried using the flow of warm air. Moreover, an induction furnace (10 °C/min) was utilized to heat up the specimens to the degree of the bonding temperature; to this end, the required pressure was simultaneously used. Accordingly, Hot Press KHP-200 furnace with the ability to create 1×10^{-3} torr vacuum was used (Figure 1). The maximum applied temperature was 1700 °C, and the dimensions of the chamber were $200\times200\times150$ mm^3. This furnace allows pressure and temperature to be simultaneously applied while creating a vacuum in the chamber. Pressure was applied by 2 hydraulic jaws embedded inside th chamber. The diameter of the upper jaw, made of hot working steel H13, of the press was 100 mm. Moreover, in order not to increase the temperature of the jaws to more than 100 °C, a cooling system was installed inside them. However, the minimum force that the press could apply was 500 kg. The furnace heating system was equipped with graphite elements, covered with a layer of compressed graphite fibers to prevent heat loss inside the furnace. Due to the significant effect of the temperature on both process and obtained results, the accuracy of the actual temperature shown by the furnace indicator was verified and calibrated using a reference thermometer (TES-1306 thermometer with K-Type thermocouple input with the acuarcy of ±3 °C). In case the lower bonding temperature was taken, no bonding between Mg and Al alloys occured due to the inadequate temperature that caused atom difussion. Of note, a decrease in the bonding presure was caused by high bonding temperature released from melting the Mg alloy. Therefore, selecting the appropriate process temperature is of significance, which is usually selected in the eutectic temperature range [8]. The proper conducted bonding times were 60 and 120 min. In case of the applied low pressure, an insufficient contact was established between the roughness of the surfaces of the samples. As a result, the chance of diffusion would be reduced. Moreover, in the presence of high pressure, the plastic deformation of the samples would occur. According to the results and experimental findings, the operational 29 MPa pressure was selected, yielding the best welding results. As the bonding was completed and just before its removal from the chamber, the samples were cooled down. A Scanning Electron Microscope (SEM) equipped with EDS/EPMA and VEGA//TESCAN-LMU was employed to study the microstructure and chemical analysis of the welding diffusion layer. It was placed in a solution containing 1/4 ml acetic acid (CH$_3$COOH), 0.6 g picric acid (C$_6$H$_3$N$_3$O$_7$), 10 ml ethanol (C$_2$H$_6$O), and distilled water (H$_2$O), in which the magnesium side was immersed for 15 s, thus being etched. However, Keller's solution was

used for etching the aluminum side. Moreover, ASTM: D1002-10 standard was used to perform shear strength test. Samples with the cross-sectional area of 10×10 mm^2 were cut by wirecut machine. Figure 2 shows the fixture used for shearing experiments. It is made of cold-rolled steel (S.P.K. 110) with hardness of 700 HV (HRC 60). Further, SANTAM STM-50 apparatus with the loading rate of 0.5 mm/min was utilized to apply the shearing force.

Figure 1. Diffusion bonding apparatues

Figure 2. Fixture designed for shearing test

Microhardness tests were performed by Vickers tester with an applied load of 50 g and a load duration of 20 s at intervals of 50 μm perpendicular to the joint. The hardness of Al 7075-T6 and Mg AZ31-O base metals was 130 and 48 HV, respectively.

3. RESULTS AND DISSCUSSION

Different specific results were obtained for welds performed at different temperatures, times, and pressures. However, the specimens welded in inappropriate conditions did not make full bonding.

Figures 3 (a-b) show that the welds performed at 38 MPa pressure and 120 min holding time and those at 80 MPa pressure and 25 min holding time, respectively, at the constant temperaturee of 393 °C, cannot make a complete joint. The Mg side was largely deformed due to the higher melting point and greater strength of A1. Furthermore, as observed in Figure 1c, due to the insufficient pressure and holding time, welding did not occur and diffusion zone was not formed. Accordingly, increasing the temperature up to 402, 412, and 421 °C and selecting the appropriate holding time (60 min) and pressure (29 MPa) would raise the possibility of diffusion of atoms and full bonding (Figure 4). The rsults from previous studies showed that the surface roughness of the contact area was an effective factor in the bonding process [14-18]. Since the surfaces are not smooth, an initial contact is witnessed between the aspirities of surfaces.
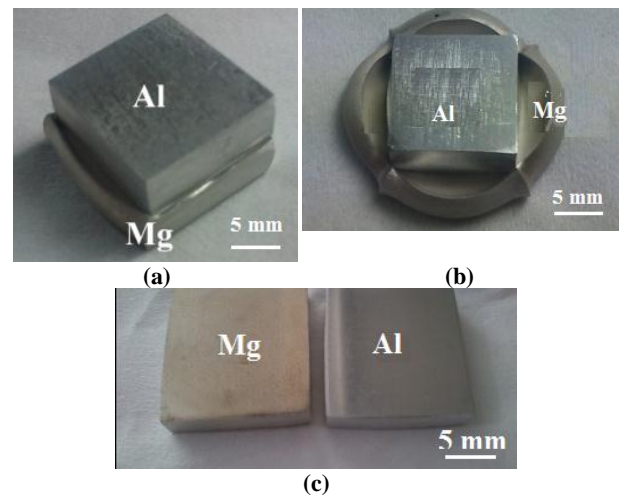

Figure 3. Unsuccessful welding with their welding conditions, a) T=393 °C, HT=120 min, P=38 MPa; b) T=393 °C, HT=25min, P=80 MPa; and c) T=402 °C, HT=30 min, P=12 MPa
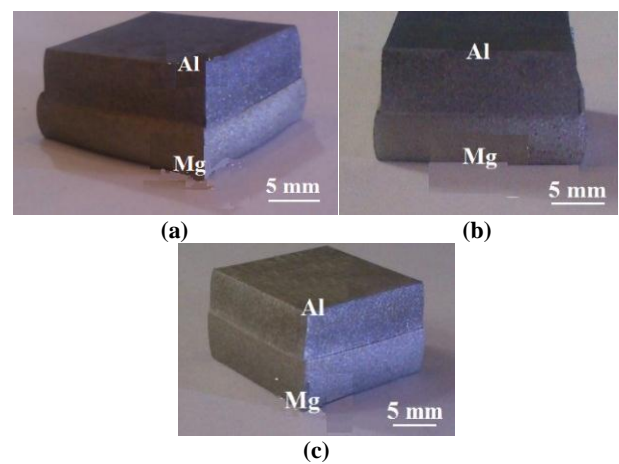
Figure 4. Successful welding with their welding conditions, a) T=402 °C, HT=60 min, P=29 MPa; b) T=412 °C, HT=60 min, P=29 MPa; and c) T=421 °C, HT=60 min, P=29 MPa

Then, an increase was observed in the contact surface of the two pieces brought about by plastic deformation and slip of roughness. Of note, at various temperatures, deformation increments and diffusion phenomenon can lead to elimination of boundaries in the interface. Finally, the filled interspaces can be observed [15]. Process temperature affects the diffusion of atoms and consequently, influences the structure of the bonding zone. Therefore, can be regarded as an effective parameter in the welding process [19, 20]. Moreover, in diffusions between two dissimilar materials, atoms with a higher diffusion coefficient diffuse faster than those with a lower diffusion coefficient [21]. The diffusion coefficients of aluminum and magnesium are equal to 1.89×10^{-12} and 2.29×10^{-12} m^2/s, respectively [9]. Therefore, more atoms diffuse across the Mg side to the Al side. This causes an imbalance in the diffusion flux and, as a result, creats voides in the bonding area. These voides, created due to the differences in the diffusion coefficient of the dissimilar materials are called Kirkendall voides, frequently referred to in the studies conducted by previous researchers [19, 21]. In a majority of the research papers investigating the dissimilar diffusion bonding, the existence of these voids was proved in the magnesium side [22]. However, in this study, Kirkendall voids were not observed through examining SEM images of the bonding zone. The difference in the diffusion coefficient of the two dissimilar materials is known as an influential parameter in the formation of the Kirkendall void, which itself depends on time and temperature. Generally, it can be concluded that the greater the difference in the diffusion coefficient, the greater the probability of the formation of Kirkendall void. Figure 5 shows the three distinct regions at the joints, performed at 402°C and 421 °C for holding time of 60 minutes. These three regions are Mg transition region (zone A), middle diffusion region (zone B), and Al transition region (zone C), respectively. The thickness of the ITZ was 21.26 μm at 402 °C, 21.96 μm at 412 °C, and 22.60 μm at 421 °C, respectively. It can be concluded that only a 19 °C increase in the temperature would lead to a 6 increase in the thickness of the ITZ. When the temperature increased, more atoms would be diffused across the interface. Hence the ITZ layer would be more thickened (Figure 6).

All samples were examined through area and linear EDS analysis. Furthermore, with the help of binary Al–Mg phase diagram, an attempt was made to determine the phases formed in the welding area (Figure 7 [23]). Figure 8 shows the linear EDS analysis of layers A, B, and C of the ITZ layer of the welded specimen at 402 °C. By examining the concentration of the elements, through both EDS analysis (Table 2) and Al-Mg binary phase diagram, it can be concluded that the layer formed on the magnesium side (layer A) comprises $Al_{12}Mg_{17}$ (γ). This phase has a BCC crystal structure with the hardness of 4.35 nHV [14]. The middle diffusion layer is a
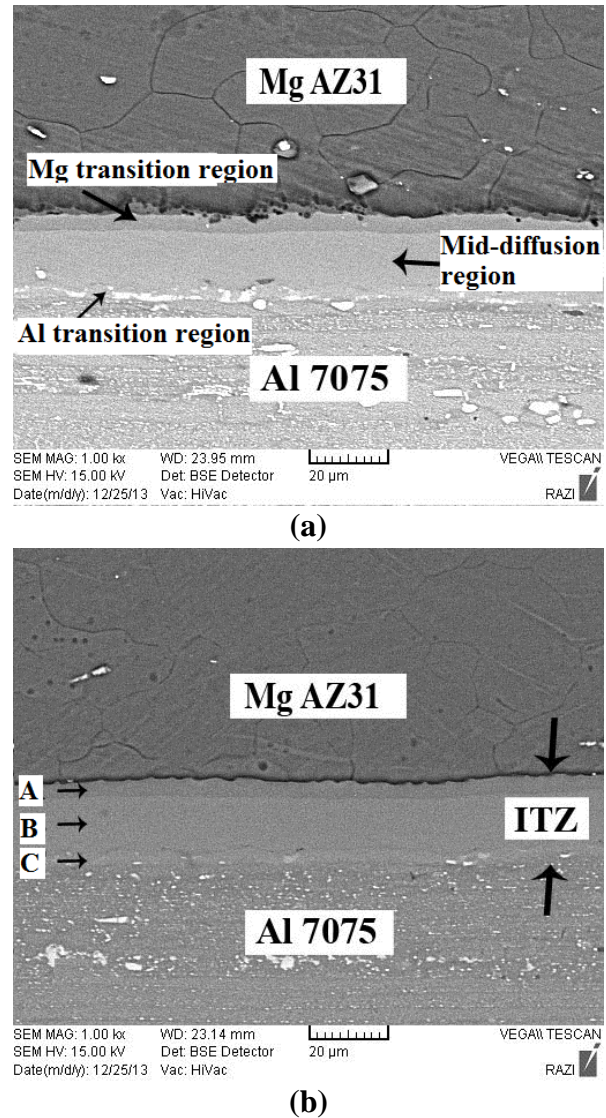

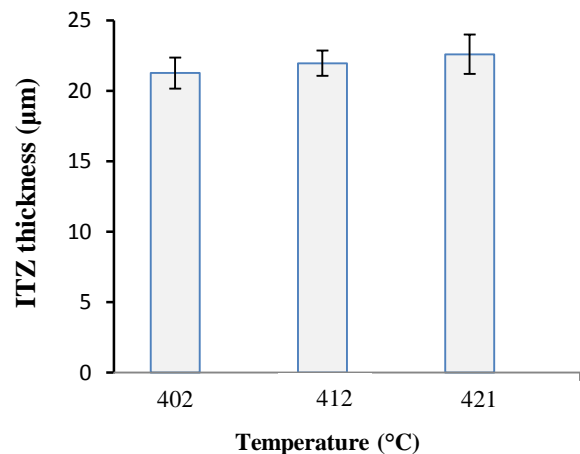**Figure 5.** SEM image of interface bonding at P=29MPa, HT=60Min and **a)**T=402°C, **b)** T=421°C

Figure 6. Effect of welding temperature on ITZ thickness

combination of phases γ and β (Al₃Mg₂), and the value for phase β on the aluminum side is greater than that on the other side. The β phase with FCC structure has the hardness of 4.4 nHV [14]. In case the diffusion welding is at its starting point, Mg and Al atoms start diffusing into the contact layer. In the next step, Al and Mg atoms diffuse into different zones and their values increase in the bonded layer. Then, a reaction occurs between them and a combination layer consisting of Al and Mg is formed. Further, as the temperature increases, the Al in Mg/MgAl interface begins to diffuse to the Mg side, the reaction $17Mg + 12Al \rightarrow Mg_{17}Al_{12}$ occurs. and $Mg_{17}Al_{12}$ is formed. As mentioned earlier, the amount of Mg in the MgAl/Al interface layer increases; and as a resutl of its diffusion through the Al side, the reaction $2Mg + 3Al \rightarrow Al_3Mg_2$ occurs and the Mg_2Al_3 phase is formed. Finally, as the process continues, there is no change in the phases and only the thickness of the ITZ layer gradually increases [9, 24]. In case of more heating, eutectic reactions $Al_{12}Mg_{17} + Mg \rightarrow L$ and $Al_3Mg_2 + Al \rightarrow L$ occur at eutectic temperature 437 °C and 450 °C, respectively. Diffusion welding is a solid-state bonding process in which the weld metal is not usually melted. To reveal the liquid formation, micrographic images can be employed to detect dendritic structures, indicating the solidification microstructure [25]. Since the operating temperatures are lower than the eutectic temperature, the liquation does not occur at the bonding zone and the intermetallic layers formed at the joint interface can be attributed to solid-state inter-diffusion of Al and Mg during diffusion bonding. It should be noted that further melting should be avoided; otherwise, it would reduce the applied pressure during the diffusion welding and then, the metal with low melting temperature would be deformed.

In the solid state processes, the formation rate of the intermetallic compunds is affacted by the rate of diffusion, which also depends on parameters such as process temperature, grain size, and other metallurgical characteristics. To form these phases, the two sides first diffuse each other and, then, a supersaturated solid solution is formed.

As the amount of elements in the solution increases, nucleation begins and intermetallic phases are formed. Then, these compounds grow longitudinally along the bonding line. In the next step, the next intermetallic compounds are formed and grown. It can be concluded that the compounds with the highest amount of an element and higher diffusion coefficient would nucleate first. Therefore, γ-$Al_{12}Mg_{17}$ is formed first [14]. In this process, the Mg diffusion activation energy in Al is lower than Al in Mg, hence Mg diffuses faster. Since the γ-$Al_{12}Mg_{17}$ phase is rich in Mg, it is formed earlier than the β-Al_3Mg_2 phase [9].

As Figure 9 illustrates, in the case of examining the diffusion element map obtained from the EDS analyses, the presence of Zn is observed in the intermetallic

bonding. Furthermore, investigation of elemental maps clarifies that the Zn diffusion area in the welding joint is massed in the Al side of the joints (Figure 10). The Zn distribution also reveals an accumulated precipitate zone at the Al_3Mg_2 aluminum alloy interface. The extraordinary growth of the Zn concentration in this zone was already expected due to the diffusion of Al in the intermetallic compounds; consequently, the formation of $MgZn_2$ precipitates occurs.
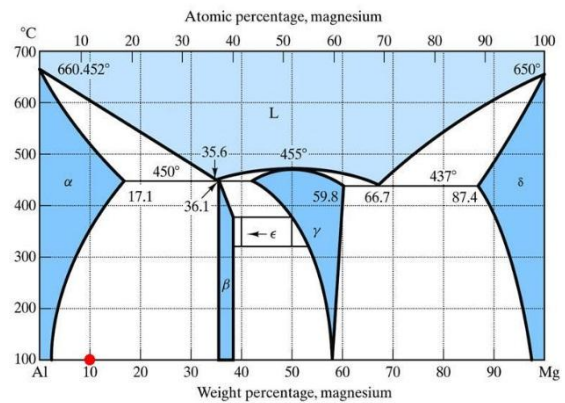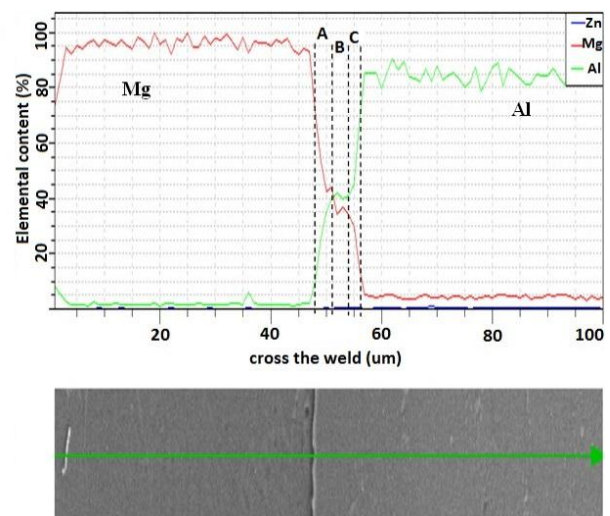

Figure 7. Binary Al-Mg phase diagram [23]

Figure 8. EDS line scan across the bonding interface as indicated by line for the specimen welded at 402 °C, P=29 MPa, and HT=60 min

TABLE 2. Basic elemental percentage in different joint zones of Figure 4b according to point analysis

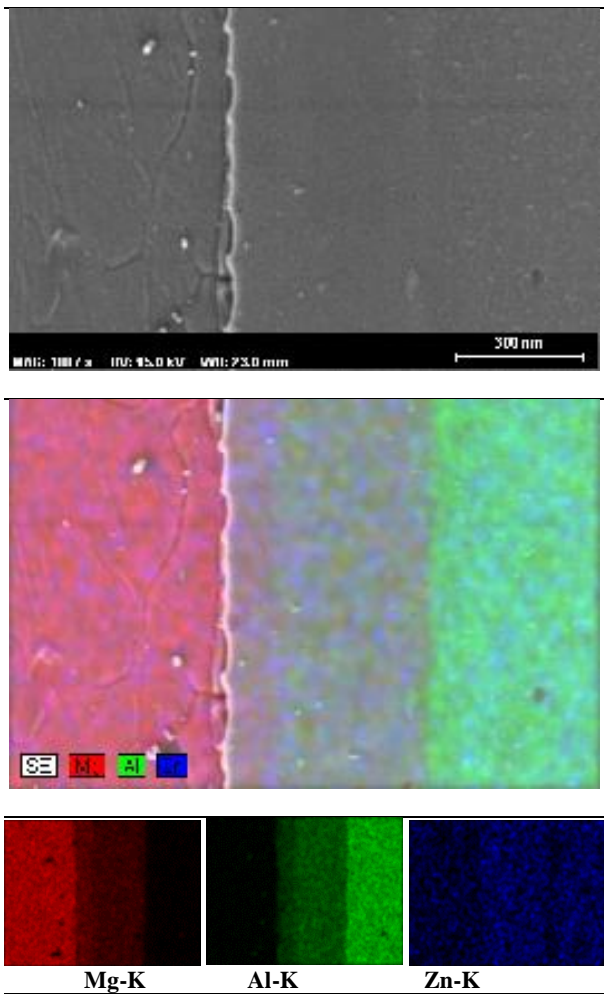|	Mg (wt. %)	Al (wt. %)	Zn (wt. %)	Cu (wt. %)
A	53.76	46.13	-	-
B	36.79	60.00	3.21	
C	22.41	73.73	2.11	1.75

Figure 9. Element map obtained from the EDS analyses for the specimen diffusion welded at 421 °C for 60 min
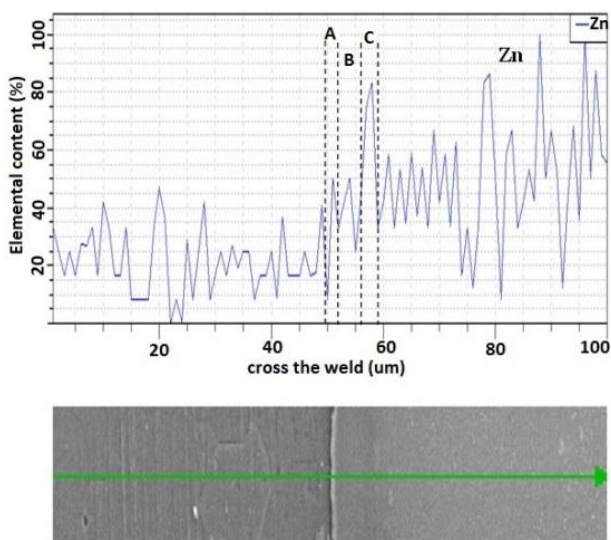

Figure 10. EDS line scan for Zn element across the bonding interface as indicated by line for the specimen welded at 421 °C, P=29 MPa and HT=60 min

Micro-hardness experiment was applied to investigate the hardness characteristics of the joint zone. The Vickers hardness on the Mg side is approximately equal to 40 HV, which increases sharply in the interface zone and then, is reduced to 60 HV on the Al side (Figure 11). Of note, increasing the temperature would lead to an increase in the microhardness in the reaction zone; however, it has no significant effect on the microhardness of base metals. In this sense, the maximum hardness in the interface reaches 90 HV and 70 HV at process temperatures of 421 °C and 402 °C, respectively. Accordingly, reduction in the amount of brittle intermetallic component formation at lower temperatures should be taken into account. Due to the presence of α-phase, the hardness of the reaction layer at 402 °C approaches the hardness of the aluminum base metal.
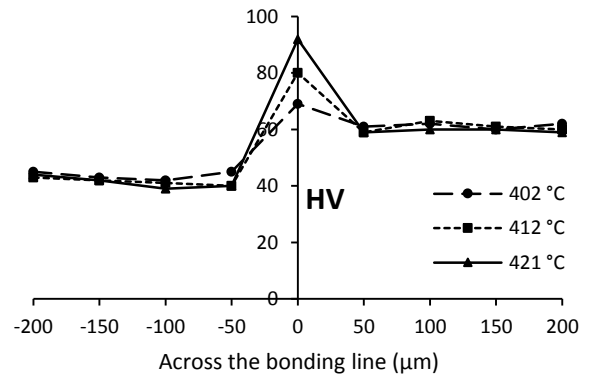

Figure 11. Effect of temperature on microhardness across the bonding line

Figure 12 shows the changes in the shear strength of welded specimens at different process temperatures. The results showed that the maximum shear stress was equal to 30 MPa at the temperature of 402 °C. In addition, at 421 °C, it reached 20 MPa. At 402 °C, the plastic deformation of the surface roughness would result in better contact of the surfaces, thus reducing the brittleness due to the formation of intermetallic phases [26]. Therefore, the bond shear strength would be considerably improved. On the contarary, by increasing the temperature to 421 °C, the amount of brittle compounds would basically increase and accordingly, the positive effect of better contact of surfaces at high temperatures would be eliminated, thus reducing the shear strength [26].

In order to simulate and investigate the effect of process parameters, diffusion welding of 7075 aluminum alloy and AZ31 magnesium alloy was simulated using Deform-3D FEM software. DEFORM-3D is capable of simulating three-dimensional material flow during the forming processes without the cost and delay of shop trials. To this end, the tetrahedral mesh type with 0.7 mm element size opted for the meshing process, and the area near to the bonding would yiled a quite fine mesh with an

element size of 0.3 mm. Furthermore, the friction coefficient was chosen to be 0.25, as suggested by DEFORM-3D software for diffusion welding process (Figure 13).
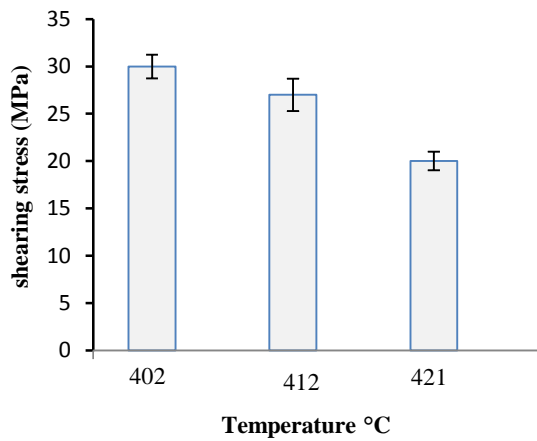

Figure 12. Effect of temperature on the welding shear strength
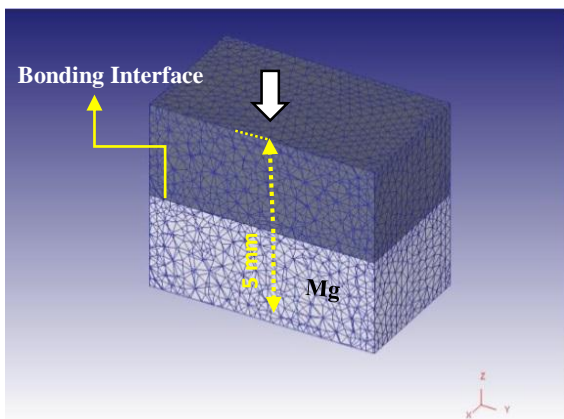

Figure 13. The initial billet meshed finite element model

Table 3 reported the thermo-mechanical properties of the used material in this study which was taken from ASTM Standards. Since the diffusion welding process is a thermo-mechanical process, the Young's module of the materials changes during the process. Table 4 reports the amounts of Young's module of 7075 aluminum alloy and AZ31 magnesium alloy at different temperatures.

TABLE 3. Mechanical and thermal properties used in this research

Parameters	Poisson Ratio	Thermal Conductivity (W/mK)	Heat Capacity (J/g°C)	Thermal E xpansion (m/m°C)
Al7075	0.33	130	0.960	23×10^{-6}
AZ31	0.35	96	1.020	25×10^{-6}

**TABLE 4.** Young's module variations of MgAZ31 and Al7075 at different temperatures

Temperature (°C)	Young's modulus (GPa)	
	MgAZ31	Al7075
100	38	68
150	32	65
200	29.8	63
250	28.9	59
450	25.9	48

The required data in this study were extracted from the experimental studies previously conducted by other researchers [27, 28]. In the next step, the extracted data of the plastic behavior (flow stress curve) of 7075 aluminum alloy and AZ31 magnesium alloy in different strain rates and temperatures were entered in DEFORM-3D software.

The effective von Mises stress was employed to determine whether or not the sample would yield the desired result during the complex loading. In this case, it can also be called the effective stress. The effective stress distribution in the deformed sample is inhomogeneous and varies based on the process temperature. The amount of effective stress close to the core of the AZ31 magnesium specimen was maximum. The highest effective stresses were 9.1, 8.8, and 7.5. MPa for temperatures at 421, 412, and 402 °C, respectively. Of note, the value for the effective stress in the 7075 aluminum, compare to the AZ31 magnesium specimen, was quite low, mainly due to the fact that Young's module of AZ31 magnesium between 402 to 421 °C was approximately two times lower than that of 7075 aluminum.

Given that the point tracing approach was employed as shown in the sectional view (Figure 13), the variation of the effective stress of 7075 aluminum and AZ31 magnesium was recored. The value for the effective stress according to the distance from the bonding interface in both materials was measured and reported in Figure 14. As observed, during the diffusion welding process, by increasing the temperature, the effective stress would gain higher values and the amount of the effective stress of AZ31 magnesium would be remarkably larger than that of 7075 aluminum. The change of effective stress across the 7075 aluminum specimen is illustrated in Figure 14a. In case the distance from the bonding interface increased, the effective stress would significantlly decrease. Moreover, Figure 14b depicts the effective stress across the bonding interface on the AZ31 magnesium side. In a distance almost equal to 0.5 mm from the bonding interface, the graph incrementally increased and then, by increasing the distance from the bonding interface, the effective stress would gradually decrease. Diffusion of Al atoms into Mg

would change the frictional force in the interface layer and cause an increase and decrease in effective stress, respectively. Therefore, changes in the range and amount of effective stress can be used as an indicator for diffusion monitoring of atoms in the welding process. As the intensity of these changes increased, more diffusion would occur and the thickness of the interface layer would be greater.
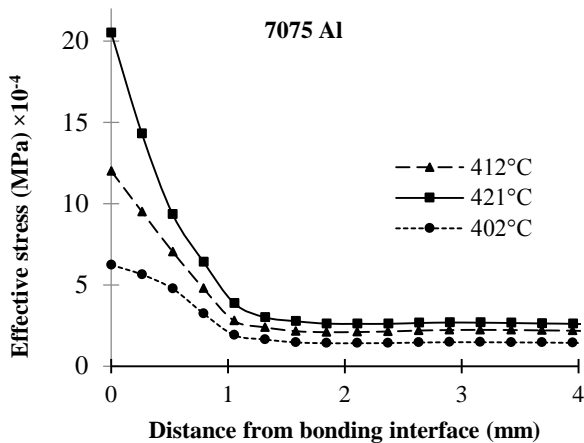
**(a)**
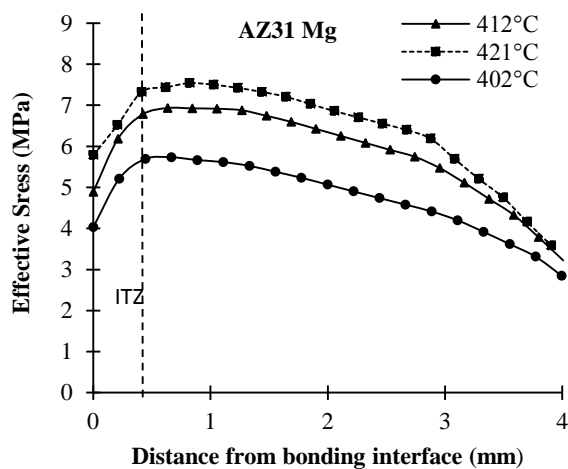
(b)

Figure 14. Effective stress according to distance from the bonding interface a- Al ; b- Mg

An experiment was performed to validate the simulation results. The diffusion welding experiment was performed at the temperature of 402 °C. The forming force was simulated during the welding process. Figure 15 shows a comparison between the welding force and hydraulic press arm stroke for the simulated and trial results. The results indicated a good agreement between the experimental results and the simulation. However, at the beginning and end of arm stroke, significant differences were observed between the simulated and experimental results. By considering the load–stroke curve, the amount of press tonnage used fot performing the diffusion welding process can be determined.
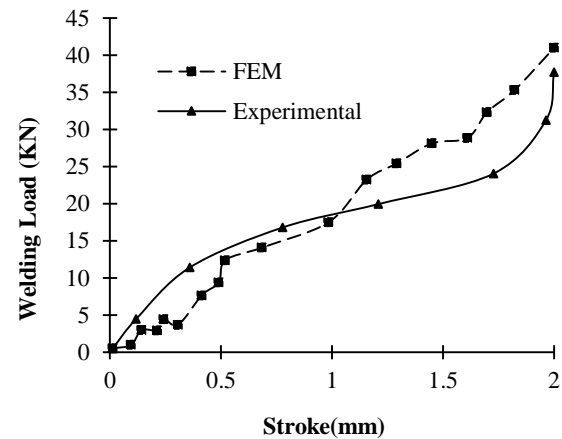
Figure 15. Comparison between the simulated and experimental load of diffusion welding process at T=402 °C

4. CONCLUSION

The present study aimed to investigate the diffusion bonding of 7075 aluminum and AZ31 magnesium alloys. To this end, the effect of different conditions such as temperature, holding time, and applied pressure during the welding process was evaluated. The results from experiments and simulations indicated that:

- Due to the insufficient temperature, pressure, and holding time for the diffusion, the bonding performed at 38 MPa and 120 min as well as at 80 MPa and 25 min could not make a full bonding (while the process temperature was kept constant at 393 °C). However, by applying the pressure, temperature, and holding time equal to 12 MPa, 402 °C, and 30 min, respectively, a complete connection was not obtained and in most areas, proper diffusion did not occur.
- As the temperature increased from 402 °C to 421 °C, more atoms diffused, resulting in a 6 increase in the thickness of the ITZ layer.
- A careful examination of the weld microstructure revealed that the formed layer from the magnesium side toward the aluminum side was composed of γ ($Al_{12}Mg_{17}$), a mixture of γ and β (Al_3Mg_2), and a mixture of γ and β with higher weight percent of β, respectively.
- On the Al side of the joints, Zn in the weld interface was denser. The significant increase in the Zn concentration in this region was due to the diffusion

of aluminum into the intermetallic phases as well as the formation of $MgZn_2$ precipitates.

- The shear strength of joints performed at 402 °C and 421 °C was 30 MPa and 20 MPa, respectively, indicating the considerable effect of increasing the process temperature on the formation of more intermetallic compounds, thus reducing the shear strength. In addition, due to the formation of more brittle phases at high temperatures, the hardness of the ITZ increased by increasing the temperature. In this regard, the maximum hardness of 90 HV was obtained during the experiments caried out at 421 °C.

- The results derived by FEM simulation were in good agreement with the experimental trials. By recording the effective stress, important information about the thermo-mechanical affected zone and thickness of the interface layer can be obatined. In other words, through the effective stress simulation, significant measures were taken in monitoring the diffusion welding process.

ACKNOWLEDGEMENTS

REFERENCES

1. Mahendran, G., Balasubramanian, V., Senthilvelan, T., "Developing diffusion bonding windows for joining AZ31B magnesium–AA2024 aluminium alloys", *Materials & Design*, Vol. 30, No. 4, (2009), 1240-1244. https://doi.org/10.1016/j.matdes.2008.06.015

2. Sun, D. Q., Gu, X. Y., Liu, W. H., "Transient liquid phase bonding of magnesium alloy (Mg–3Al–1Zn) using aluminium interlayer", *Materials Science and Engineering: A*, Vol. 391, No.1-2, (2005), 29-33. https://doi.org/10.1016/j.msea.2004.06.008

3. Aydın, K., Kaya, Y., Kahraman, N., "Experimental study of diffusion welding/bonding of titanium to copper", *Materials & Design*, Vol. 37, (2012), 356-368. https://doi.org/10.1016/j.matdes.2012.01.026

4. Guo, Y., Qiao, G., Jian, W., Zhi, X., "Microstructure and tensile behavior of Cu-Al multi-layered composites prepared by plasma activated sintering", *Materials Science and Engineering: A*, Vol. 527, No. 20, (2010), 5234-5240. https://doi.org/10.1016/j.msea.2010.04.080

5. Nami, H., Halvaee, A., Adgi, H., Hadian, A., "Microstructure and mechanical properties of diffusion bonded Al/Mg_2Si metal matrix in situ composite", *Materials & Design*, Vol. 31, No. 8, (2010), 3908-3914. https://doi.org/10.1016/j.matdes.2010.03.007

6. Hadian, R., Emamy, M., Varahram, N., Nemati, N., "The effect of Li on the tensile properties of cast Al–Mg_2Si metal matrix composite", *Materials Science and Engineering: A*, Vol. 490, No. 1-2, (2008), 250-257. https://doi.org/10.1016/j.msea.2008.01.039

7. Somekawa, H., Watanabe, H., Mukai, T., Higashi, K., "Low temperature diffusion bonding in a superplastic AZ31 magnesium alloy", *Scripta Materialia*, Vol. 48, No. 9, (2003), 1249-1254. https://doi.org/10.1016/S1359-6462(03)00054-X

8. Fernandus, M. J., Senthilkumar, T., Balasubramanian, V., "Developing Temperature–Time and Pressure–Time diagrams for diffusion bonding AZ80 magnesium and AA6061 aluminium alloys", *Materials & Design*, Vol. 32, No. 3, (2011), 1651-1656. https://doi.org/10.1016/j.matdes.2010.10.011

9. Jafarian, M., Khodabandeh, A., Manafi, S., "Evaluation of diffusion welding of 6061 aluminum and AZ31 magnesium alloys without using an interlayer", *Materials & Design (1980-2015)*, Vol. 65, (2015), 160-64. https://doi.org/10.1016/j.matdes.2014.09.020

10. Samanta, A., Xiao, S., Shen, N., Li, J., Ding, H., "Atomistic simulation of diffusion bonding of dissimilar materials undergoing ultrasonic welding", *The International Journal of Advanced Manufacturing Technology*, Vol. 103, No. 1, (2019), 879-890. https://doi.org/10.1007/s00170-019-03582-9

11. Kumar, S. S. S., Ravisankar, B., Sheriff, M. A., Silvister, M. J., "Thermal Analysis of Dissimilar Materials Diffusion Bonding Using Finite Element Method", In *Materials Science Forum*, Vol. 969, (2019), 858-863. Trans Tech Publications Ltd. https://doi.org/10.4028/www.scientific.net/MSF.969.858

12. Ding, Y., Ju, D., "Finite Element Analysis of Residual Stress in the Diffusion Zone of Mg/Al Alloys", *Advances in Materials Science and Engineering*, Vol. 2018, (2018), 1-8. https://doi.org/10.1155/2018/1209849

13. Mahendran, G., Balasubramanian, V., Senthilvelan, T., "Mechanical and metallurgical properties of diffusion bonded AA2024 Al and AZ31B Mg", *Advances in Materials Research: AMR*, Vol. 1, No. 2, (2012), 147-160. https://doi.org/10.12989/amr.2012.1.2.147

14. Zhang, M. X., Huang, H., Spencer, K., Shi, Y. N., "Nanomechanics of Mg–Al intermetallic compounds", *Surface and Coatings Technology*, Vol. 204, No. 14, (2010), 2118-2122. https://doi.org/10.1016/j.surfcoat.2009.11.031

15. Zuruzi, A. S., Li, H., Dong, G., "Effects of surface roughness on the diffusion bonding of Al alloy 6061 in air", *Materials Science and Engineering: A*, Vol. 270, No. 2, (1999), 244-248. https://doi.org/10.1016/S0921-5093(99)00188-4

16. Derby, B., Wallach, E. R., "Theoretical model for diffusion bonding", *Metal Science*, Vol. 16, No. 1, (1982), 49-56. https://doi.org/10.1179/030634582790427028

17. Derby, B., Wallach, E. R., "Diffusion bonding: development of theoretical model", *Metal Science*, Vol. 18, No. 9, (1984), 427-431. https://doi.org/10.1179/030634584790419809

18. Elzey, D. M., Wadley, H. N. G., "Modeling the densification of metal matrix composite monotape", *Acta Metallurgica et Materialia*, Vol. 41, No. 8, (1993), 2297-2316. https://doi.org/10.1016/0956-7151(93)90312-G

19. Zhang, J., Shen, Q., Luo, G., Li, M., Zhang, L., "Microstructure and bonding strength of diffusion welding of Mo/Cu joints with Ni interlayer", *Materials & Design*, Vol. 39, (2012), 81-86. https://doi.org/10.1016/j.matdes.2012.02.032

20. Mofid, M. A., Loryaei, E., "Investigating microstructural evolution at the interface of friction stir weld and diffusion bond of Al and Mg alloys", *Journal of Materials Research and Technology*, Vol. 8, No. 5, (2019), 3872-3877. https://doi.org/10.1016/j.jmrt.2019.06.049

21. Srinivasan, D., Subramanian, P. R., "Kirkendall porosity during thermal treatment of Mo–Cu nanomultilayers", *Materials Science and Engineering: A*, Vol. 459, No. 1-2, (2007), 145-150. https://doi.org/10.1016/j.msea.2007.01.037

22. Gao, M., Mei, S., Li, X., Zeng, X., "Characterization and formation mechanism of laser-welded Mg and Al alloys using Ti interlayer", *Scripta Materialia*, Vol. 67, No. 2, (2012), 193-196. https://doi.org/10.1016/j.scriptamat.2012.04.015

23. Liu, L., Ren, D., "A novel weld-bonding hybrid process for joining Mg alloy and Al alloy", *Materials & Design*, Vol. 32, No. 7, (2011), 3730-3735. https://doi.org/10.1016/j.matdes.2011.03.050

24. Wang, J., Yajiang, L., Wanqun, H., "Interface microstructure and diffusion kinetics in diffusion bonded Mg/Al joint", *Reaction Kinetics and Catalysis Letters*, Vol. 95, No. 1, (2008), 71-79. https://doi.org/10.1007/s11144-008-5259-9

25. Firouzdor, V., Kou, S., "Formation of Liquid and Intermetallics in Al-to-Mg Friction Stir Welding", *Metallurgical and Materials Transactions A*, Vol. 41, No. 12, (2010), 3238-3251. https://doi.org/10.1007/s11661-010-0366-4

26. Mahendran, G., Balasubramanian, V., Senthilvelan, T., "Influences of diffusion bonding process parameters on bond characteristics of Mg-Cu dissimilar joints", *Transactions of Nonferrous Metals Society of China*, Vol. 20, No. 6, (2010), 997-1005. https://doi.org/10.1016/S1003-6326(09)60248-X

27. Li, Y., Wu, Z., "Microstructural Characteristics and Mechanical Properties of 2205/AZ31B Laminates Fabricated by Explosive Welding", *Metal*, Vol. 7, No. 4, (2017), 125. https://doi.org/10.3390/met7040125

28. Mei, R., Bao, L., Cai, B., Li, C., Liu, X., "Piecewise modeling of flow stress of 7075-T6 aluminum alloy in hot deformation", *Materials Transactions*, Vol. 57, No. 7, (2016), 1147-1155. https://doi.org/10.2320/matertrans.M2015465